J Electroceram (2008) 21:851–854
DOI 10.1007/s10832-008-9506-2

DC conduction behavior of $Bi_{3.15}Nd_{0.85}Ti_3O_{12}$ thin films grown by RF-magnetron sputtering

Hai-Joon Lee · Chang Won Ahn · Sun Hee Kang · Chang Do Kim · Ill-Won Kim · Jin Soo Kim · Jeong Sik Lee

Received: 27 June 2005 / Accepted: 28 December 2005 / Published online: 29 April 2008
© Springer Science + Business Media, LLC 2008

Abstract The $Bi_{3.15}Nd_{0.85}Ti_3O_{12}$ (BNT) thin films were deposited on Pt(111)/Ti/SiO_2/Si substrates by using RF-magnetron sputtering method and studied the ferroelectric and leakage current charateristics. The polarization – electric field (*P-E*) hysteresis loops of BNT film was well saturated with the remnant polarization ($2P_r$) of 29.8 μC/cm^2 and a coercive field ($2E_c$) of 121 kV/cm. The leakage current density – electric field (*J-E*) characteristics of the Pt/BNT/Pt capacitor reveals the presence of two conduction region, having Ohmic behavior at low electric field (below 50 kV/cm) and Schottky-emission or Poole-Frenkel emission at high electric field (above 60 kV/cm). The barrier height and trapped level of BNT films are estimated to be 1.11 eV and 0.90 eV, respectively.

Keywords $Bi_{3.15}Nd_{0.85}Ti_3O_{12}$ · Conductivity · Ferroelectricity · RF-magnetron sputtering

1 Introduction

The ferroelectric and electrical properties of bismuth layer structured ferroelectrics, such as $SrBi_2Ta_2O_9$(SBT), and $Bi_4Ti_3O_{12}$ (BIT), have been intensively investigated for applications of non-volatile memory devices [1]. The $Bi_4Ti_3O_{12}$ single crystal exhibited a large spontaneous polarization and piezoelectric constants. The polarization axis of BIT lies in the *a-b* plane at an angle of about 4.5° to the *a*-axis. Hence there is a *c*-axis (P_r ~ 4 μC/cm^2) and an *a*-axis (P_r ~ 50 μC/cm^2) component of polarization [2]. However, the thin films and ceramics of BIT suffer from high leakage current and deteriorating physical properties due to lattice defects and randomly oriented grains. Recently, lanthanum and neodymium substituted BIT films were reported to have a relatively large $2P_r$~24 μC/cm^2 and excellent fatigue resistance. Kojima et al. [3] and Watanabe et al. [4] reported that $Bi_{3.54}Nd_{0.46}Ti_3O_{12}$ and $Bi_{3.35}Nd_{0.65}Ti_3O_{12}$ thin films prepared by metal-organic chemical vapor deposition had large $2P_r$ value of 25 and 34 μC/cm^2, respectively. Zhang et al. [5] reported that the $Bi_{3.15}Nd_{0.85}Ti_3O_{12}$ thin film fabricated by pulsed laser deposition showed relatively small value of 8.8 μC/cm^2. Wu et al. [6] and Chon et al. [7] reported that the BNT thin films prepared by sol-gel process showed various $2P_r$ values of 17~103 μC/cm^2. The reasons of various $2P_r$ values for BNT films were the difference of chemical composition, deposition method and grain orientations.

In generally, the current density – electric field characteristics, at the low field region, are Ohmic nature. In the high field region, different conduction mechanisms, e.g., Schottky, Poole-Frenkel, and space charge limited conduction were verified to explain the true nature of charge transport phenomena in BLSFs films [8, 9].

Schottky emission mechanism is an electrode limited conduction, where the entire leakage current is dominated by the Schottky barrier generated at the interface of the electrode and film. Contrary to the electrode-limited conduction, the Poole–Frenkel mechanism is a bulk limited

H.-J. Lee · C. W. Ahn · S. H. Kang · C. D. Kim · I.-W. Kim (✉)
Department of Physics, University of Ulsan,
Ulsan 680–749, South Korea
e-mail: kimiw@mail.ulsan.ac.kr

J. S. Kim
Research Center for Dielectric and Advanced Matter Physics,
Pusan National University,
Busan 609–735, South Korea

J. S. Lee
Department of Physics, Kyungsung University,
Busan 608–736, South Korea

charge transport in the insulating thin film. It is recognized in terms of lowering the potential barrier of the trap levels during the application of an external electric field.

The previous reports were focused on the enhancement of ferroelectric properties of Nd substituted BIT films. However, there has been no report on the conduction characteristics of BNT films. In this study, we report ferroelectric and conduction behavior of $Bi_{3.15}Nd_{0.85}Ti_3O_{12}$ thin films fabricated by RF-magnetron sputtering.

2 Experiment

The RF-magnetron sputtering system was used to fabricate $Bi_4Ti_3O_{12}$ (BIT) and $Bi_{3.15}Nd_{0.85}Ti_3O_{12}$ (BNT) thin films from the ceramic target. For the ceramic targets, 10 mole% Bi excess $Bi_4Ti_3O_{12}$ and $Bi_{3.15}Nd_{0.85}Ti_3O_{12}$ ceramics were prepared by solid state reaction method. The BIT and BNT films were deposited on Pt(111)/Ti/SiO_2/Si(100) substrates at 450°C. The thickness of Pt and Ti films were 150 nm and 10 nm, respectively. The films were deposited the operating partial pressure of 110 mTorr and sputtering time of 4 hrs, which was maintained the RF power of 60 W (~ 3 W/cm^2). The film thickness of both BIT and BNT were 750 nm. The BNT thin films were annealed at 700°C in air ambient for 1 hrs. The compositions of BIT and BNT films measured by energy dispersive spectrometer (EDS) were $Bi_{3.99}Ti_{2.87}O_{12+\delta}$ and $Bi_{3.17}Nd_{0.82}Ti_{2.90}O_{12+\delta}$, respectively. The crystalline structure and surface morphology were obtained using X-ray diffraction (XRD) and atomic force microscope (AFM), respectively. In order to study the electrical properties, Pt electrodes were deposited by using DC sputtering. The ferroelectric *P-E* hysteresis loops were measured using RT66A (Radiant Technology, USA). The leakage current – voltage (*I-V*) characteristics were analyzed using Keithley-237 electrometer (Keithley Inc., USA) at the temperature range from room temperature to 200°C.

3 Results and discussion

Figure 1 shows the XRD patterns of BIT and BNT thin films annealed at 700°C in air ambience. The BIT thin films exhibited (00*l*) diffractions, whereas BNT thin film revealed random orientation with a (117) peak. When the rare earth ions with the smaller ion radius such as Nd, Sm and Gd are substituted into the BIT, the orientation of these films was changed because of the increased lattice mismatch between the (111) plane of Pt on Ti/SiO_2/Si substrate and (00*l*) plane of BIT with the substitution of rare-earth ion with the smaller ionic radius. The ionic radii of Bi^{3+} and Nd^{3+} are 0.135 nm and 0.127 nm, respectively [10]. Thus, the BNT thin film showed random orientation with the enhanced (117) reflection.

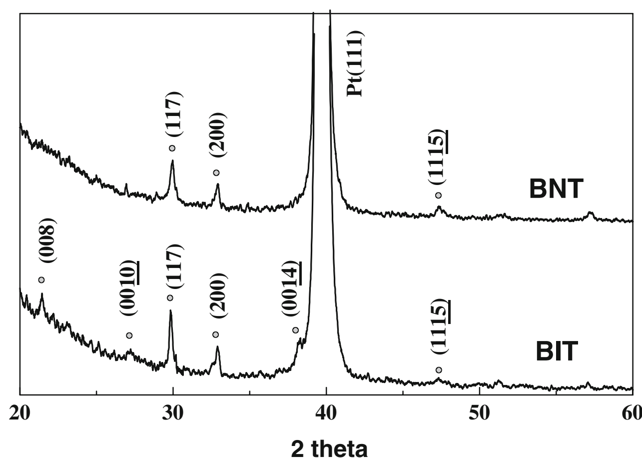

Fig. 1 XRD patterns of BIT and BNT thin films

Figure 2 show *P-E* hysteresis loops of the BIT and BNT thin films annealed at 700°C in air ambience. The *P-E* hysteresis loops of BIT thin film was not saturated and it showed very leaky shape. This behavior is related to leakage current property. Otherwise, at an applied field of about 200 kV/cm, the $2P_r$ and $2E_c$ values of BNT film are obtained 29.83 μC/cm^2 and 121.7 kV/cm, respectively. The structural ferroelectricity is known to be based upon the distortion of the atom from the original position along one axis. Generally, the main axis of BIT system thin films for ferroelectricity was considered to be *a*-axis. Therefore, the large remnant polarization value of BNT thin film compared with that of BIT is probably caused by the difference in the crystal orientations between the two kinds of films.

Figure 3 shows the behavior of leakage current density of BIT and BNT thin films as a function of applied field (*J-E* plot) at room temperature. The *J-E* curves of both films can be divided into 3 regions. For BNT film, the first region is from 0 to 47 kV/cm, the second one from 47 kV/cm to 75 kV/cm, and the third one above 75 kV/cm. In the first region, the leakage current increases slightly with increasing applied field. The rate of increase in the second region with a higher bias is larger than that of the first region. The third region shows dielectric breakdown in both films. In practice, third region should be ignored when analyzing the conduction mechanism. The values of n in the figure is the exponent in the relation $J=cE^n$, where c is constant. In the low field region, values of n are around 1, which implies Ohmic conduction. For BIT film, the leakage current density reached to dielectric breakdown at this region. On the other hand, BNT film has a complex conduction mechanism in second region.

In this study, the conduction mechanism of BNT thin film was determined by fitting the experimental data into the Schottky and Poole-Frenkel models. Figure 4 shows the *J-E* characteristics of BNT film as a function of the applied field at the temperature range from room temperature to

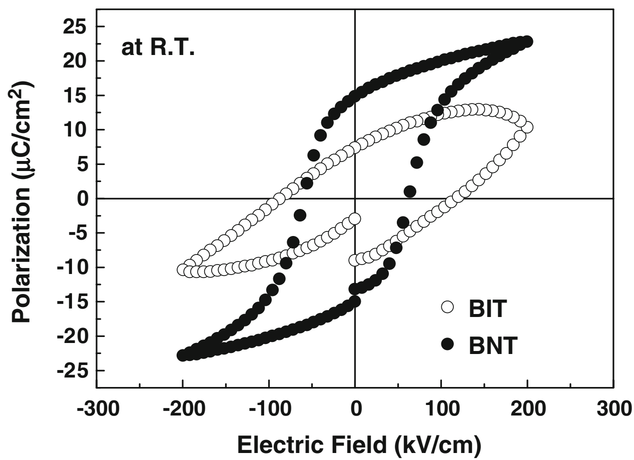

Fig. 2 *P-E* hysteresis loops of BIT and BNT thin films

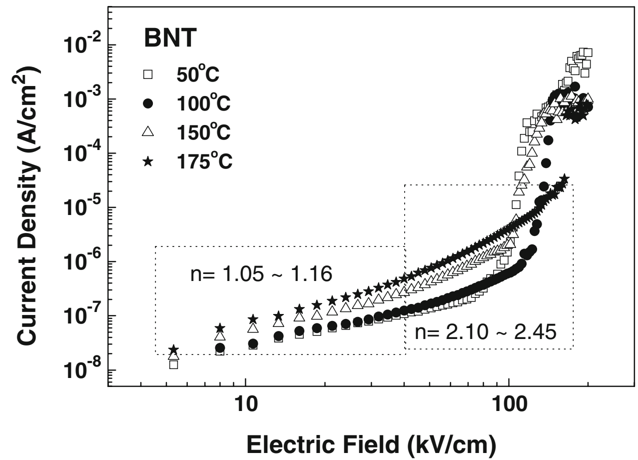

Fig. 4 Leakage current characteristics of BNT thin film with different temperatures

175°C. For BNT film, the leakage current densities slightly increased with increasing temperatures and the slopes are increased from 1.05 to 1.16, below 40 kV/cm. In this region, *J-E* characteristic exhibits Ohmic behavior. At the high field region above 40 kV/cm, the slopes are increased from 2.10 to 2.45.

Figure 5(a) shows the variation of the log(J/T^2) at the applied field ranging from 64 to 100 kV/cm and the inverse of the temperature (insert figure) according to the Schottky emission model. The current density expression for Schottky emission was given by [8],

$$\ln J/T^2 = \frac{q\phi_B + q\sqrt{qE/4\pi\varepsilon_i}}{kT} + \ln A^* \quad (1)$$

where ϕ_B, q, k, T, ε_i, and A^* are the interface potential barrier height, electric charge, Boltzmann's constant, absolute temperature, permittivity of insulator, and Richardson constant, respectively. The barrier height of BNT film was estimated to be 1.11 eV and associated with the oxygen vacancy migration. Kim et al. [11] reported the leakage current characteristics of La doped BIT ($Bi_{3.25}La_{0.75}Ti_3O_{12}$: BLT) thin films fabricated by sol-gel process and explained that the leakage current behavior of BLT thin film was followed by Schottky emission model, and calculated barrier height was 1.06 eV. Ezhilvalavan et al. [12] reported that the conduction mechanism of sputtered $SrBi_2(V,Nb)_2O_9$

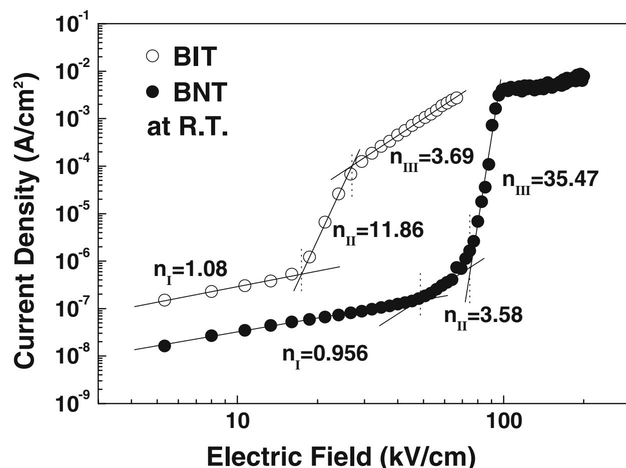

Fig. 3 Current density (*J*) – electric field (*E*) curves of BIT and BNT thin films

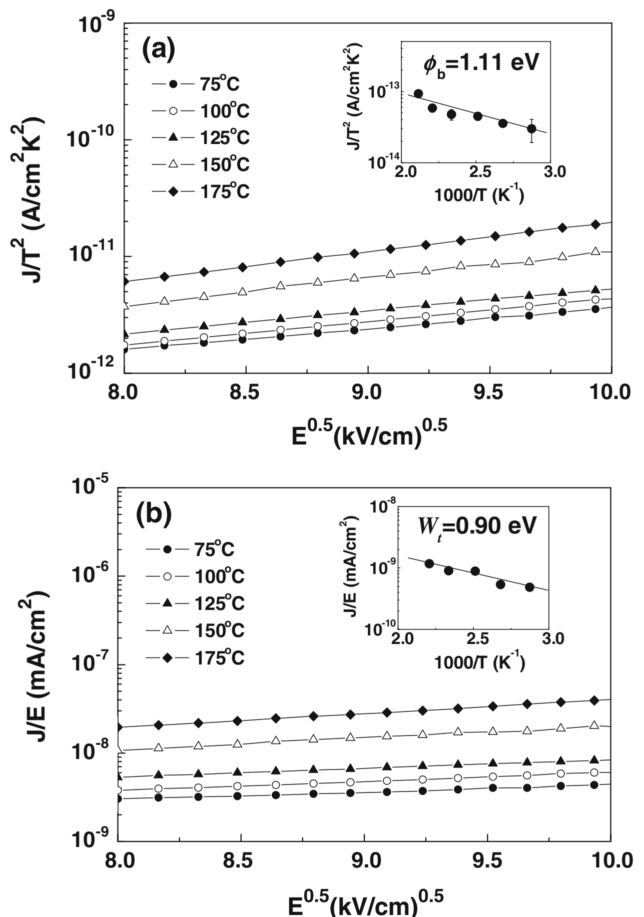

Fig. 5 (a) J/T^2 vs $E^{0.5}$ plot for Schottky emission fitting and (b) J/E vs $E^{0.5}$ plot for Poole-Frenkel emission fitting

(SBVN) thin film with Pt electrode was followed Schottky and Poole-Frenkel emission models. The barrier height at interface of between SBVN film and Pt electrode was 1.39 eV.

The current density expression for Poole-Frenkel emission was given by [8],

$$\ln J/E = -\frac{qW_t + q\sqrt{qE/\pi\varepsilon_i}}{kT} + \ln C \tag{2}$$

where W_t is the trapped center level and C is a constant.

The level of trapped center was 0.9 eV as shown in the inset of Fig. 5(b), which was extracted from the extrapolated value at $E=0$. This value was similar to the conductance activation energy of BLT thin film and implies that the conduction behavior was governed by the same conduction mechanism [13].

Doubly charged oxygen vacancies were considered to be the most mobile charges in perovskite ferroelectrics and play an important role in the conduction process [14, 15]. The activation energy of oxygen vacancies in $SrTiO_3$ was 1.0~1.1 eV, and that in $PbTiO_3$-based materials was 0.9~1.1 eV [16, 17]. The activation energy value observed from BNT thin film is consistent with the activation energy of oxygen vacancy in other perovskite materials, which confirms that the conductance and tapped center of BNT thin film is determined by oxygen vacancies.

In this study, it is very difficult to prove which conduction mechanism among Poole-Frenkel and Schottky emission models is suitable for BNT film. The barrier hight analyzed from Schottky emission model and trapped level from Poole-Frenkel emission model for BNT film were 1.11 eV and 0.90 eV, respectively. The actual conduction mechanism of BNT film may be a mixture of both Schottky and Poole-Frenkel emission.

4 Conclusions

The *P-E* hysteresis loops of $Bi_{3.15}Nd_{0.85}Ti_3O_{12}$ thin film showed well saturated rectangular shape with $2P_r$ and $2E_c$ of 29.83 $\mu C/cm^2$ and 121.7 kV/cm, respectively. The slope of log(*J*)-log(*E*) plot at low electric field for BNT films are around 1, which implies Ohmic conduction. The BNT film has a complex conduction mechanism at the intermediate region. At higher electric field region, the conduction in BNT thin film can be explained by both Schottky and Poole-Frenkel emission models. From a Schottky emission plot, the barrier height of BNT film was estimated to be 1.11 eV. The trap center was calculated using Poole-Frenkel emission, and the value for BNT was 0.90 eV. The conductance and tapped center of BNT thin film is probably controlled by oxygen vacancies.

Acknowledgments This work was supported by No. R05–2003–000–11584–0 from Basic Research Program of the Korea Science and Engineering Foundation.

References

1. J.F. Scott, C.A. Araujo, Science **246**, 1400 (1989)
2. S.E. Cummins, L.E. Cross, J. Appl. Phys. **39**, 2268 (1968)
3. T. Kojima, T. Sakai, T. Watanabe, H. Funakubo, Appl. Phys. Lett. **80**, 2746 (2002)
4. T. Watanabe, T. Kojima, T. Sakai, H. Funakubo, M. Osada, Y. Noguchi, M. Miyayana, J. Appl. Phys. **92**, 1518 (2002)
5. S.T. Zhang, X.J. Zhang, H.W. Cheng, Y.F. Chen, Z.G. Liu, N.B. Ming, X.B. Hu, Y.J. Wang, Appl. Phys. Lett. **83**, 4378 (2003)
6. D. Wu, Y. Xia, A. Li, Z. Liu, N. Ming, J. Appl. Phys. **94**, 7376 (2003)
7. U. Chon, H.M. Jang, M.G. Kim, C.H. Chang, Phys. Rev. Lett. **89**, 087601 (2002)
8. S.M. Sze, *Physics of Semiconductor Devices* (John Wiley & Sons, New York, 1981), p. 402
9. A. Laha, S.B. Krupanidhi, J. Appl. Phys. **92**, 415 (2002)
10. M. Yamasa, N. Iizawa, T. Yamaguchi, W. Sakamoto, K. Kikuta, T. Yogo, T. Hayashi, S. Hirano, Jnp. J. Appl. Phys. **42**, 5222 (2003)
11. K.T. Kim, C.I. Kim, *Surf. Coat. Technol.* **177**, 774 (2004)
12. S. Ezhilvalavan, V. Samper, T.W. Seng, X. Junmin, J. Wang, J. Appl. Phys. **96**, 2181 (2004)
13. D. Wu, A. Li, N. Ming, Appl. Phys. Lett. **84**, 4505 (2004)
14. S. Saha, S.B. Krupanidhi, J. Appl. Phys. **87**, 849 (2000)
15. I.W. Kim, C.W. Ahn, J.S. Kim, T.K. Song, J.S. Bae, B.C. Choi, J. H. Jeong, J.S. Lee, Appl. Phys. Lett. **80**, 4006 (2002)
16. R. Waser, J. Am. Ceram. Soc. **74**, 1934 (1991)
17. W.L. Warren, K. Vanheusden, D. Dimos, G.E. Pike, B.A. Tuttle, J. Am. Ceram. Soc. **79**, 536 (1996)